Effect of Dissociation Equilibria on Ion-Exchange Processes of Weak Electrolytes

Marcel L. Jansen, Joop Houwers, Adrie J. J. Straathof, Luuk A. M. van der Wielen, Karel Ch. A. M. Luyben, and Will J. J. van den Tweel
Dept. of Biochemical Engineering, Delft University of Technology, Julianalaan 67, 2628 BC Delft, The Netherlands

Ion-exchange processes involving weak electrolytes are influenced strongly by the pH via the occurrence of association/dissociation equilibria. This influence was investigated quantitatively through binary displacement experiments with different electrolytes to gain better insight in the role of the pH and to test a fixed-bed ion-exchange model used for the description of multicomponent processes. The two major factors determining the ion-exchange behavior of weak electrolytes are the actual exchange of counterions and the sorption of neutral species. The sorption of neutral species resulted in concentration fluctuations superimposed on the normal ion-exchange profiles, whereas pH fluctuations inherent to ion-exchange processes in general also influenced concentration through modified ionic fractions. The relative importance of these contributions is determined by the magnitude of parameters such as resin capacity, distribution coefficients of neutral species, and selectivities of ions, as well as by operating conditions such as concentrations of all species.

Introduction

Ion-exchange chromatography is one of the major processes for the separation of charged components. Due to the presence of undissociated species, ion-exchange processes of weak electrolytes are more complex than processes involving only strong electrolytes. Models for ion exchange that have been set up for strong electrolytes (Fóti et al., 1994; Myers and Byington, 1986) are not applicable to weak electrolytes since they do not take the partitioning of the nonionic species into account. In other models that have been set up for weak electrolyte systems, the active participation of neutral species in the exchange process has often been neglected (Helfferich and Bennett, 1984a,b; Saunders et al., 1989; Jones and Carta, 1993; Kitakawa et al., 1994). In later work, Helfferich considered the uptake of weak electrolytes by ion-exchange resins to be a superposition of the exchange of ions and a linear uptake of undissociated species (Helferrich, 1990). This theory was adopted by Tao (1995). Jansen et al. (1996a), following the approach of Kawakita and Matsuishi (1991), have derived a rigorous ion-exchange model from basic thermodynamic equilibrium relations. This Donnan Ion eXchange equilibrium model (DIX model) not only describes the usual exchange of counterions but it also takes the uptake of coions and neutral species into account. For dilute solutions the model was shown to be converging to conventional models as far as the uptake of counterions is concerned.

The basis for chromatographic processes is the equilibrium distribution of components between a mobile and a stationary phase. Secondary equilibria occur if, in addition to the phase equilibria, the concentration and/or form of an involved species is chemically altered. Then the distribution becomes a function of the normal distribution and of the chemical equilibrium. In contrast to our previous work, where the ion-exchange equilibrium is treated as a phase equilibrium (Jansen et al., 1996a), ion exchange is usually considered as a chemical reaction. The term "secondary *chemical* equilibria" is then used instead. An extensive treatise of secondary (chemical) equilibria in chromatography is given by Karger et al. (1980). It is well known that chemical reactions may affect the behavior of weak electrolytes in chromatographic and related processes. Keller and Giddings (1960) discussed the occurrence of multiple spots arising from a single component in

Correspondence concerning this article should be addressed to L. A. M. van der Wielen.
Current addresses of: M. L. Jansen, Diosynth b.v., P.O. Box 20, 5340 BH Oss, The Netherlands; W. J. J. van den Tweel, DSM Andeno, P.O. Box 81, 5900 AB Venlo, The Netherlands.

paper chromatography. They mentioned chemical equilibria, including dissociation equilibria and complexation, as possible sources of multiple spots. Peak splitting of a single component into two distinct peaks connected by a zone of low concentration of the same substance is also known in capillary electrophoresis (Ermakov et al., 1994). The basis of this phenomenon is the presence of a charged and uncharged form of the same substance, the former moving electrophoretically and the latter driven by electroosmosis. Similar phenomena, the more or less independent behavior of different ionic forms of a single component, were also observed in anion-exchange processes with weak acids (Jansen et al., 1996b).

Scope and objective

In a previous article a rigorous ion-exchange equilibrium model (Jansen et al., 1996a) was incorporated in a fixed-bed model in order to describe the dynamic behavior of ion-exchange columns (Jansen et al., 1996b). The dynamic model was applied to single-component processes and verified experimentally for the weak electrolytes *N*-acetylmethionine and acetic acid. In the present study the model is applied to aqueous solutions containing more than one solute. The attention is focused on systems containing chloride and/or the weak electrolytes acetic acid and *N*-acetylmethionine. A mixture of the latter components plus L-methionine results from the enantioselective enzymatic hydrolysis of *N*-acetyl-DL-methionine. This reaction is employed for the industrial production of enantiomerically pure L-methionine, where acetic acid is a byproduct and *N*-acetyl-D-methionine remains unconverted (Wandrey and Flaschel, 1979; Chibata and Tosa, 1976). The separation of these compounds is therefore of considerable commercial interest. This acylase process is one of the most important processes for the industrial production of L-amino acids in general. The work presented here is part of a study to develop a chromatographic reactor in which the just-mentioned reaction is integrated with a first chromatographic separation step of the reaction mixture (Jansen et al., in preparation).

It was shown previously that the uptake of neutral species, in addition to the uptake of ions, has a considerable effect on the behavior of single-component ion-exchange processes and that the pH plays an important role. Preliminary studies with two-component systems demonstrated that displacement of one weak electrolyte by another led to concentration fluctuations that were assumed to have the same origin as the phenomena observed in single-component processes. This assumption will be tested in the present study for two-component systems in which chloride, acetic acid, and *N*-acetylmethionine are involved. For that purpose experiments will be performed in which one electrolyte is displaced by another, and simulations will be done with the dynamic fixed-bed ion exchange model. The attention is focused on two factors that are related to the occurrence of dissociation equilibria. On the one hand, there is a reduction of the retention of weak electrolytes if its ionic fraction is reduced by the transition into the neutral form. On the other hand, the retention is increased by the uptake of the neutral species. The net effect of these factors is investigated in this study, with emphasis on the pH and the degree of dissociation or the strength of the weak electrolytes. A third factor, that becomes important at high electrolyte concentrations, is the additional uptake of coions, but this is irrelevant for the relatively low concentrations applied in this work.

Modeling and simulation

The DIX equilibrium model used in this study has been described in detail elsewhere (Jansen et al., 1996a). The resulting equation for the equilibrium concentrations of univalent counterions in the resin phase reads as follows:

$$c_a^R = c_a^L S_{a,\mathrm{OH}^-} \cdot \frac{Q + \sqrt{Q^2 + 4AC}}{2A} \tag{1}$$

with auxiliary functions A and C defined as:

$$A = \sum_a c_a^L S_{a,\mathrm{OH}^-} \qquad C = \sum_c c_c^L S_{c,\mathrm{H}^+} \tag{2}$$

Here c is the concentration, S is the selectivity, Q is the resin capacity, index a denotes anions, c cations, R the resin phase, and L the liquid phase. The selectivity between two univalent ions a and b is defined as follows:

$$S_{a,b} = \frac{c_a^R}{c_a^L} \frac{c_b^L}{c_b^R}. \tag{3}$$

The resin phase concentration of univalent coions (here cations) is given by

$$c_c^R = c_c^L S_{c,\mathrm{H}^+} \cdot \frac{2A}{Q + \sqrt{Q^2 + 4AC}}. \tag{4}$$

In this respect the model differs from traditional ion-exchange models. It describes the uptake of coions, whereas traditional ion-exchange models assume complete exclusion of coions due to the Donnan effect (Helfferich, 1962). For neutral species i a linear relation between resin-phase and liquid-phase concentrations with an overall distribution coefficient, K_i, was derived (Jansen et al., 1996a):

$$c_i^R = c_i^L \cdot K_i. \tag{5}$$

This equation applies to all neutral species, including undissociated weak acids or bases as well as net neutral zwitterions, like many amino acids in solution. As shown in the Appendix, this distribution coefficient can be related simply to the resin-phase-dissociation constant, which cannot be measured directly. Linear uptake of neutral components was also proposed by Helfferich (1990), whose theory was adopted by Tao (1995). In other ion-exchange models, the resin-phase concentrations of these species are often related to the ionic concentrations via the dissociation constants (Kawakita and Matsuishi, 1991; Mehablia et al., 1994). If different forms of a single component coexist, for example, an anionic, cationic, and/or neutral form, the total uptake of that component by the resin is given by the sum of the contributions of Eqs. 1, 4, and 5.

The dynamic fixed-bed model is based on a differential mass balance for each component over a fixed bed, assuming plug-flow with axial dispersion (Jansen et al., 1996b):

$$\frac{\partial c_i^L}{\partial \theta} + \frac{(1-\epsilon)}{\epsilon}\frac{\partial c_i^R}{\partial \theta} + \frac{\partial c_i^L}{\partial z} - \frac{1}{Pe}\frac{\partial^2 c_i^L}{\partial z^2} = 0. \quad (6)$$

Here θ is the dimensionless time, ϵ is the void fraction of the bed, z is the dimensionless longitudinal coordinate, Pe is the Péclet number, $u_o L/\epsilon D$, with u_0 the superficial velocity, L the column length and D the dispersion coefficient. If internal and/or external mass-transfer limitations exist, these effects are lumped together with axial dispersion to give an apparent dispersion coefficient. The Péclet number then comprises mass-transfer effects as well. In general this lumping works well if mass transfer and diffusion are not too important, but models in which mass transfer is incorporated explicitly could also be used (Guiochon et al., 1994). Assuming local equilibrium and using the chain rule, the changes in time of resin- and liquid-phase concentrations are related as follows:

$$\frac{\partial c_i^R}{\partial \theta} = \sum_{j=1}^{n} \frac{\partial c_i^R}{\partial c_j^L}\frac{\partial c_j^L}{\partial \theta}, \quad (7)$$

where n is the number of components. Substitution of this equation into the mass balance, Eq. 6, gives, after some minor rearrangements, the following equation (in vector notation):

$$(I_n + \beta\Gamma)\frac{\partial \mathbf{c}^L}{\partial \theta} + \frac{\partial \mathbf{c}^L}{\partial z} - \frac{1}{Pe}\frac{\partial^2 \mathbf{c}^L}{\partial z^2} = \mathbf{0}. \quad (8)$$

Here I_n is the n-dimensional identity matrix, Γ is the Jacobian matrix of partial derivatives, with $\Gamma_{i,j} = \partial c_i^R/\partial c_j^L$, $\mathbf{c}$ is the vector of concentrations, and β is the volume ratio of resin and liquid phases, $(1-\epsilon)/\epsilon$. The set of differential equations is solved by backwards discretization of the space variable using finite differences and Taylor expansion (Carta et al., 1988; DeCarli et al., 1990; Golshan-Shirazi and Guiochon, 1992; Guiochon et al., 1994):

$$\frac{1}{\Delta z}(\mathbf{c}_k^L - \mathbf{c}_{k-1}^L) = \frac{\partial \mathbf{c}_k^L}{\partial z} - \frac{\Delta z}{2!}\frac{\partial^2 \mathbf{c}_k^L}{\partial z^2} + \frac{\Delta z^2}{3!}\frac{\partial^3 \mathbf{c}_k^L}{\partial z^3} - \cdots, \quad (9)$$

where $1/\Delta z$ equals the number of spatial discretization steps, and index k denotes the kth discretization step. Using only the first term in this Taylor expansion series, the error is of the order of Δz, and the coefficient of this error is the second-order partial differential, $\partial^2 \mathbf{c}_k^L/\partial z^2$. The second-order term in Eq. 8 is eliminated through substitution of actual dispersion by numerical dispersion, using the appropriate number of discretization steps, N (Guiochon et al., 1994):

$$N = \frac{1}{\Delta z} = \frac{Pe}{2}. \quad (10)$$

The following equation is then obtained for the variation of the concentrations in time:

$$\frac{\partial \mathbf{c}_k^L}{\partial \theta} = -\frac{1}{\Delta z}(I_n + \beta\Gamma)^{-1}(\mathbf{c}_k^L - \mathbf{c}_{k-1}^L). \quad (11)$$

The course of the concentrations as a function of time is obtained by numerical integration of this equation with a fourth-order Runge-Kutta algorithm.

Materials and Methods

Chemicals

Acetic acid and sodium chloride (analytical grade) were obtained from Baker, Deventer, The Netherlands. *N*-acetyl-DL-methionine and DL-methionine were obtained from Sigma, St. Louis, MO. Hydrochloric acid and sodium hydroxide solutions (analytical grade) were obtained from Merck, Darmstadt, Germany. Arginine monohydrochloride was obtained from Mann, New York. The strong-base, macroporous, hydrophilic ion-exchange resin Macro-Prep Q was obtained from Bio-Rad, Hercules, CA.

Analyses

Off-line analyses of acetic acid and *N*-acetylmethionine were done by HPLC on a Bio-Rad HPX-87H column of 7.8 mm internal diameter and 30 cm in length, operating at 60°C, with UV detection at 210 nm. The eluent was a 10-mM phosphoric acid solution of pH 2 at a flow rate of 0.6 mL/min. Chloride was determined with a chloride-specific Orion model 96-17B combination chloride electrode (Orion, Boston, MA).

Column characterization

A fixed bed of Macro-Prep Q resin with a bed length of 6.0 cm was prepared in a glass column with an internal diameter of 1.5 cm; the total bed volume was 10.60 mL. The dead volume of the system and the effective void fraction of the bed were determined by pulse-response analysis using arginine as inert tracer at a concentration of 10 mmol/L dissolved in 10 mmol/L hydrochloric acid with an eluent of 10 mM hydrochloric acid. The dead volume in tubes and detectors was determined from the results of experiments with zero bed height. The void fraction was calculated from the total bed volume and the difference between total liquid volume and dead volume of the system.

The ion-exchange capacity of the bed was determined by equilibration of the bed with a 0.1-M sodium hydroxide solution and subsequent washing with deionized water to remove the excess OH^-. Then this bed was equilibrated with a 0.1-M hydrochloric acid solution until breakthrough occurred, and washed with deionized water. The effluent of the equilibration step with hydrochloric acid and the subsequent washing step was collected and titrated with a 1-M sodium hydroxide solution. The bed capacity was recalculated from the amount of hydrochloric acid fed to the column and the excess amount found with the back-titration.

Displacement experiments

The column was equilibrated with a 100-mM solution of an electrolyte (eluent *A*, see Table 1). At $t = 0$ the eluent was replaced by a solution of another electrolyte (eluent *B*) of

Table 1. Applied Electrolytes and Experimental Conditions for the Displacement Experiments

Electrolyte System Eluent $A \rightarrow$ Eluent $B \rightarrow$ Eluent A	pH Eluent A	pH Eluent B	Flow Rate (mL/min)	Dimensionless Block Width
Ac → AcM → Ac	6.98	7.05	1.221	10.111
AcM → Cl → AcM	5.02	5.04	1.225	10.114
Ac → Cl → Ac	4.91	5.04	1.206	9.987
Ac → AcM → Ac	4.89	5.02	1.251	10.359

equal molarity and approximately equal pH. After 50 min the feed was switched back to the original eluent A and the column was equilibrated with eluent A for another 50 min. The applied electrolytes and the precise experimental conditions are given in Table 1. Although the feed concentration of the electrolytes was always 100 mmol/L, the sodium concentration was sometimes lower due to incomplete dissociation of the acid. For acetic acid at pH 5 the sodium concentration was 64 mmol/L and for *N*-acetylmethionine at pH 5 this was 97 mmol/L; in all other solutions the sodium concentration was higher than 99.5 mmol/L. In view of the intended separation of acetic acid and *N*-acetylmethionine in a chromatographic reactor with immobilized aminoacylase, the minimum pH in this study was 5, which is about the lower limit for enzymatic activity (Jansen et al., 1996c).

The process was monitored on-line with an Ultrospec III spectrophotometer (Pharmacia LKB, Uppsala, Sweden) with variable wavelength, a Consort K720 conductivity meter (Consort, Turnhout, Belgium), and a pH meter (Model 691, Metrohm, Herisau, Switzerland). The experimental setup is represented in Figure 1. Eighty effluent samples with a sample time of 75 s, corresponding to a sample volume of 1.51–1.56 mL, were taken using a fraction collector (Model 2110, Bio-Rad, Richmond, CA). Effluent samples were analyzed off-line to determine acetate, *N*-acetylmethionine, and chloride concentrations.

The influence of the pulse width was investigated with a prepacked Econo-Pac Q resin cartridge of 5 mL at a flow rate of 1.5 mL/min. Block pulses of 100 mmol/L *N*-acetylmethionine on a column equilibrated with acetic acid at pH 5 were given. The applied pulse widths were 15, 25, and 35 min. The effluent was analyzed only on-line using a pH meter (Model 691, Metrohm, Herisau, Switzerland) and a UV monitor at 254 nm (Model EM-1, Bio-Rad, Richmond, CA).

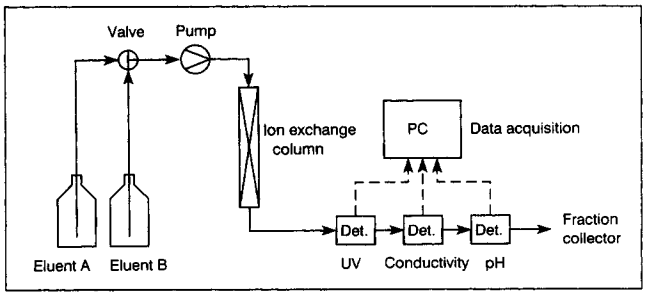

Figure 1. Experimental setup for the displacement experiments.

Results and Discussion

Column characteristics

From pulse-response analyses performed in quadruplicate a value of 10.56 ± 0.16 mL was found for the total liquid volume in the system between injection valve and UV-detector. From experiments in quadruplicate with zero bed height a value of 4.52 ± 0.022 mL was found for the dead volume. From these results a bed void fraction of 0.569 ± 0.017 was calculated. The given estimated errors are based on a 99% confidence region. The influence of the dead volume on the concentration profiles was negligible. From the results of the pulse-response experiments (not shown), it was found that most of the dispersion occurred in the column itself and not in the appendages and tubings.

The ion-exchange capacity was determined in triplicate and a value of 1.84 ± 0.063 mmol was found for the total ion-exchange capacity of the column. This corresponds to a capacity of the resin phase equal to 0.40 ± 0.03 mol/L.

Displacement experiments

Displacement experiments were performed at four different conditions (see Table 1). According to a duplicate the experiments were well reproducible. The results of the experiments are discussed below in order of increasing complexity.

Acetate/N-Acetylmethionine at pH 7. The results of the displacement of acetate by *N*-acetylmethionine and vice versa at pH 7 are presented in Figure 2. In the figure the measured and simulated profiles of the pH and the total concentration of acetate and *N*-acetylmethionine are given as functions of the dimensionless time. The dimensionless time, θ, is defined such that the retention time of the eluent equals unity:

$$\theta = t \Big/ \left(\frac{\epsilon V}{\Phi} \right). \tag{12}$$

Here V is the column volume and Φ is the flow rate.

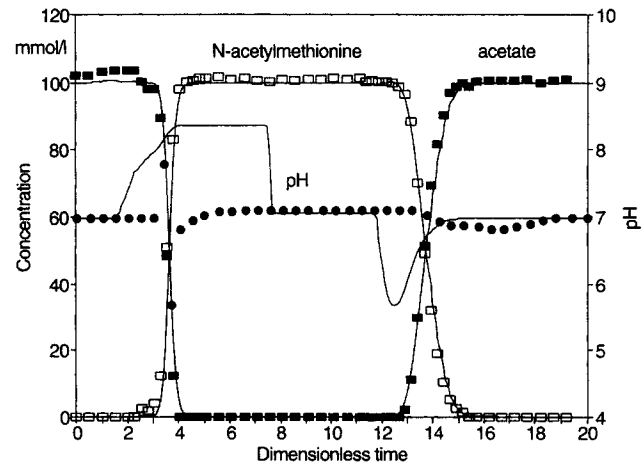

Figure 2. Response of a column equilibrated with acetate to a block pulse of *N*-acetylmethionine at pH 7.

Markers represent measurements; lines represent simulations. See Table 1 for experimental conditions.

At pH 7 only 0.6% of the total amount of acetate and 0.03% of *N*-acetylmethionine are present in the neutral form. The difference in the sodium concentration of both solutions is therefore negligible, so the two solutions differ only in the type of anion. After the introduction of *N*-acetylmethionine on the column, a wave in which acetate is being displaced by *N*-acetylmethionine starts to move through the column. Because of the presence of only two almost completely dissociated components, the response observed in the effluent at the end of the column resembles that of two exchanging strong electrolyte ions. The breakthrough of *N*-acetylmethionine is accompanied by a rise of the pH. Because $S_{AcM^-,OH^-} > S_{Ac^-,OH^-}$ (Jansen et al., 1996a; see also the section titled "Simulations), Eq. 1 predicts that more *N*-acetylmethionine than acetate is taken up when they are at the same liquid-phase concentration. Also, as a consequence some OH^- is displaced by *N*-acetylmethionine. This results in an excess of OH^- in the liquid phase and thus in a pH increase of the effluent.

Similarly, the pH decreases again after the step back from *N*-acetylmethionine to acetate. The deficiency of OH^- on the resin is replenished with OH^- from the liquid. The observed steepness of the wave of acetate exchanging against *N*-acetylmethionine is somewhat less than that of the first wave of *N*-acetylmethionine exchanging against acetate. This confirms that the value of the selectivity of *N*-acetylmethionine over OH^- is higher than that of acetate over OH^-, which means that $S_{AcM^-,Ac^-} > 1$. It can be concluded from the simulations that the value is approximately equal to 1.2.

N-Acetylmethionine/Chloride at pH 5. Chloride is a strong electrolyte existing only as anion. At pH 5, *N*-acetylmethionine is still almost completely dissociated—about 3% is in the neutral form—and is supposed to behave as a strong electrolyte. However, as we have seen earlier, the displacement of one strong electrolyte anion by another may be accompanied by pH fluctuations if the mutual selectivity is not equal to 1. Because in this case a downwards pH fluctuation leads to an increased fraction of the neutral form of *N*-acetylmethionine, such a fluctuation can influence the ion-exchange process of chloride and *N*-acetylmethionine.

The concentration profiles of the effluent after a block pulse of chloride to a column initially in equilibrium with *N*-acetylmethionine, both at a pH of approximately 5, are presented in Figure 3. Because $S_{Cl^-,OH^-} > S_{AcM^-,OH^-}$ (Jansen et al., 1996a; see the section titled "Simulations"), the displacement of *N*-acetylmethionine by chloride leads to the release of OH^- from the resin (comparable to the case of acetate/*N*-acetylmethionine). Due to the pH rise, the fraction of neutral *N*-acetylmethionine becomes negligible. Therefore the first wave corresponds to the exchange of two strong anions.

The step back to *N*-acetylmethionine leads to a pH decrease to about pH 4.4 according to the simulation. At that pH about 12% of *N*-acetylmethionine is converted into the neutral form, and only 88% is present as the anion that competes with the chloride ion for the exchange sites. As a consequence *N*-acetylmethionine has lost some of its capability to displace chloride. The concentration profiles are therefore less steep than expected on the basis of the selectivity of *N*-acetylmethionine over chloride. The pH decrease has thus led here to an apparent decrease of the selectivity.

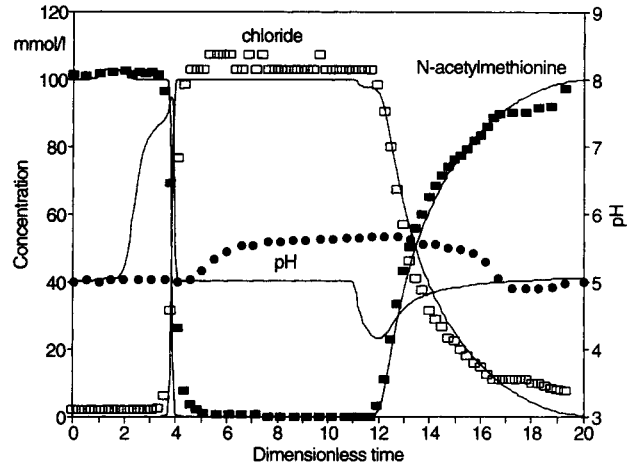

Figure 3. Response of a column equilibrated with *N*-acetylmethionine to a block pulse of chloride at pH 5.

Markers represent measurements; lines represent simulations. See Table 1 for experimental conditions.

Acetate/Chloride at pH 5. Since acetic acid is less acidic than *N*-acetylmethionine, a larger fraction is present in the undissociated form (35% at pH 5). In Figure 4 the influence of such a larger fraction on the elution profiles is illustrated by the response of a column in equilibrium with acetic acid at pH 5 to a block pulse of chloride. Although the pH and concentration of both eluents were approximately equal, serious pH fluctuations but also concentration fluctuations were observed. These concentration fluctuations are superimposed on the regular ion-exchange profiles and are so large that they can only be explained by mechanisms other than ion exchange. In previous work similar fluctuations were observed in single-component systems (with only one solute) where the pH or concentration was varied (Jansen et al., 1996b). They were attributed to interactions of uncharged species with the resin.

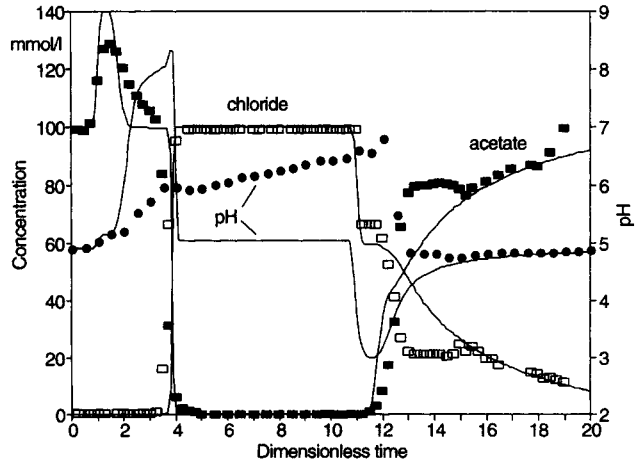

Figure 4. Response of a column equilibrated with acetate to a block pulse of chloride at pH 5.

Markers represent measurements; lines represent simulations. See Table 1 for experimental conditions.

Table 2. System Definition for the Description of the Acetate/Chloride Displacement Experiments with the Wave-Velocity Concept

Conc. Variables Resin and Liquid Phase	Equilibrium Relations and Constraints
$2\times H^+$	$2\times$ Water dissociation equilibrium (resin and liquid)
$2\times OH^-$	Acetic acid dissociation in liquid phase
$2\times Na^+$	Undissociated acetic acid distribution
$2\times Ac^-$	Selectivity Ac^-/OH^-
$2\times HAc$	Selectivity Cl^-/OH^-
$2\times Cl^-$	Selectivity Na^+/H^+
	$2\times$ Electroneutrality (resin and liquid)
Total 12	Total 9

The most striking phenomenon in Figure 4 is the appearance, before the breakthrough of chloride, of an acetic acid peak with a concentration in excess of the influent concentration, although the influent concentrations of acetate and chloride were the same. Despite the fact that only 65% is present at the acetate anion, the concentration of this anion in the initial state was sufficient to replace practically all OH^- from the resin and convert it completely into the acetate form. The lower acetate anion fraction is thus not a reason for the observed acetic acid peak. Apparently additional acetate, present on the column as neutral acetic acid, is also displaced by chloride. The total amount of ionically bound acetate and absorbed neutral acetic acid exceeds the resin capacity, Q, and therefore the effluent concentration exceeds the original 100 mmol/L in the mobile phase.

This result can also be explained qualitatively in terms of concentration waves for ion-exchange systems with reacting species (Klein, 1981; Helfferich and Bennett, 1984a,b). According to Klein's theory, the variance of the system, defined by the number of concentration variables minus the number of equilibrium relations and constraints, is equal to 3 (see Table 2). This means that three concentration waves can be expected for a step change, or a total of six waves for the block pulse.

Although the solute concentration was kept constant, the concentration of associated sodium ions was not. Because acetic acid is only partially dissociated at pH 5, the concentration of associated sodium in the acetic acid/acetate solution is less than that in the chloride solution. The introduction of chloride on the column thus brings about an increase of the sodium concentration in the column. Sodium is for the greater part excluded from the resin due to the Donnan effect, and moves through the column approximately at the liquid-phase velocity. In order to maintain electroneutrality this sodium wave is accompanied by acetate anions, which results in the increase of the conductivity after approximately one residence time (not shown). For the same reason as described in the previous cases the introduction of chloride results in the increase of the pH. Consequently, the distribution equilibrium of undissociated acetic acid is disturbed and acetic acid is released from the resin. The combination of these factors leads to an increase of the effluent concentration of acetic acid, exceeding the influent concentration of 100 mmol/L. The second wave is caused by the elution of undissociated acetic acid. After the release of undissociated acetic acid from the resin due to the changed liquid-phase composition and pH, acetic acid starts to migrate at a velocity somewhat lower than that of the mobile phase because it is slightly retained by the resin. Because the neutral acid does not contribute to the conductivity, the conductivity of the effluent remains the same. The wave becomes visible by the decrease of the effluent concentration of acetic acid until the original level of 100 mmol/L has been reached. Only the third wave relates to the actual exchange process of acetate and chloride ions. When this wave reaches the end of the column, the acetic acid/acetate concentration in the effluent drops to zero and chloride breaks through. This wave is the slowest of the three waves associated with the step from acetate to chloride.

The switch back to acetate at the end of the block pulse of chloride leads to a decrease of the sodium concentration in the influent. The sodium wave, in order to maintain electroneutrality, drags along chloride and the chloride concentration drops rapidly. Until that moment, undissociated acetic acid is taken up by the resin, enhanced by the drop of the pH. Until the undissociated acetic acid reaches the end of the column, the acetate concentration remains zero, but after that it rapidly increases. It is followed by a slower wave of acetate anions exchanging against chloride. The latter process proceeds slowly, much slower than expected on the basis of the value of the selectivity of chloride over acetate, due to the reduced acetate anion fraction as a consequence of the low pH. At the calculated pH minimum of 3, only 2% is left as acetate anion.

Acetate/N-Acetylmethionine at pH 5. The most complex of the "two-component" systems studied here is that of acetate and *N*-acetylmethionine at pH 5. *N*-acetylmethionine can exist in three forms, whereas chloride exists only as anion; here the total number of species besides water thus equals 8. A complete system definition and an analysis of its variance is given in Table 3. Despite the larger number of components, the variance is not changed because the number of relations is increased accordingly. The additional components are neutral and cationic *N*-acetylmethionine (in both phases), and the supplementary relations are the two dissociation equilibria, the distribution coefficient for the neutral species and a selectivity for the cation.

Table 3. System Definition for the Description of the Acetate/*N*-acetylmethionine Displacement Experiments with the Wave-Velocity Concept

Conc. Variables Resin and Liquid Phase	Equilibrium Relations and Constraints
$2\times H^+$	$2\times$ Water dissociation equilibrium (resin and liquid)
$2\times OH^-$	Acetic acid dissociation in liquid phase
$2\times Na^+$	$2\times$ *N*-Acetylmethionine dissociation in liquid phase
$2\times Ac^-$	Undissociated acetic acid distribution
$2\times HAc$	Undissociated *N*-acetylmethionine distribution
$2\times AcM^-$	Selectivity Ac^-/OH^-
$2\times AcM^0$	Selectivity AcM^-/OH^-
$2\times AcM^+$	Selectivity Na^+/H^+
	Selectivity AcM^+/H^+
	$2\times$ Electroneutrality (resin and liquid)
Total 16	Total 13

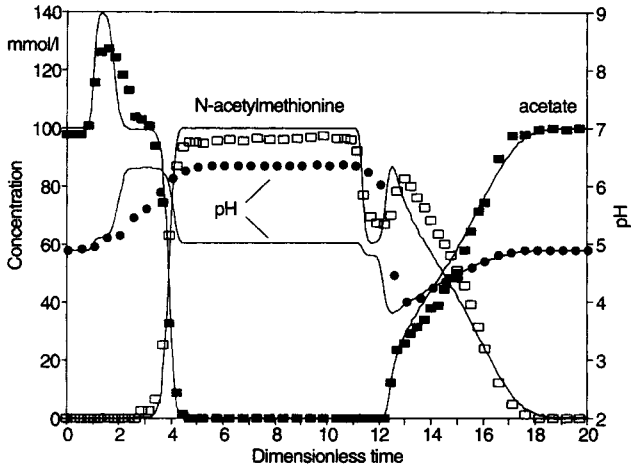

Figure 5. Response of a column equilibrated with acetate to a block pulse of *N*-acetylmethionine at pH 5.

Markers represent measurements; lines represent simulations. See Table 1 for experimental conditions.

Despite the increased complexity, again three waves per step are to be expected. This is shown in Figure 5. The first wave is the sodium wave, in combination with acetate, resulting in the increase of the total effluent concentration of acetate. The second wave is again the wave of undissociated acetic acid, and the third wave is that of *N*-acetylmethionine exchanging against acetate ions. So far the response is almost identical to that of the acetate/chloride system because *N*-acetylmethionine, like chloride, is completely anionic.

The major difference is in the step back from *N*-acetylmethionine to acetate. Reintroducing acetate leads to a decrease of the sodium concentration. In order to maintain electroneutrality, sodium leaving the column drags along *N*-acetylmethionine, which results in a rapid decrease of *N*-acetylmethionine in the effluent. Subsequently a slower wave of undissociated acetic acid moves through the column, followed by a zone in which acetate and *N*-acetylmethionine are exchanging. *N*-Acetylmethionine that is released in this way is pushed forward, helped by a partial transition into the neutral form due to the pH decrease. Therefore its concentration in the effluent temporarily increases again. Almost simultaneously undissociated acetic acid breaks through. Only when the actual ion-exchange zone reaches the end of the column, the acetate concentration increases further and the *N*-acetylmethionine concentration decreases to zero. Then the pH returns slowly to the initial value. The slopes of the acetate and *N*-acetylmethionine concentration profiles in the second exchange zone are less steep than may be expected solely on the basis of the selectivity of *N*-acetylmethionine over acetate, which is somewhat higher than 1. The drop of the pH to a value of about 4 has turned approximately 85% of the total amount of acetate into the neutral form. The remaining 15% is not very efficient in displacing *N*-acetylmethionine which is for about 25% in its neutral form. The reduced competitiveness of acetate is obvious after comparison of these results with those obtained with the same electrolytes at pH 7 where both components were completely dissociated (see above).

Simulations with the fixed-bed chromatography model

The simulations, briefly mentioned earlier, to test the validity of the dynamic chromatography model based on the DIX equilibrium model are now discussed in detail. The parameters used in the simulations were based on results from previous equilibrium studies, from dynamic experiments with single-component systems (Jansen et al., 1996a,b) and from this work. Some of the parameter values were slightly adapted to obtain a better agreement between simulated and measured profiles. This is explained below. Without rigorously optimizing all parameter values at the same time, one single set of parameters was used to simulate all experiments. With this set in general a very good agreement between experimental concentration profiles and simulated profiles was obtained. A survey of the parameter values is given in Table 4.

Based on the Péclet number of 270 that followed from the pulse-response experiments (result not shown), the number of 135 discretization steps is calculated from Eq. 10. To reduce calculation time we have used 100 discretization steps, because further increasing the number did not noticeably improve the simulated profiles. In order to make the model more predictive instead of correlative, we have minimized the experimental input by using only parameters from the equilibrium experiments. Therefore the pH profile was computed as well, although the measured profile could have been used as experimental input.

Resin Capacity. The breakthrough time of a block pulse is strongly determined by the capacity, Q. For low electrolyte concentrations (small values of A and C in Eq. 2) the breakthrough time is proportional to the capacity. Within the limits of its 99% confidence region, the value of the resin capacity was modified from 0.40 to 0.375 mol/L in order to obtain a better agreement between experiments and simulations. Nevertheless, the capacity still seems to be overestimated a little in the acetate/*N*-acetylmethionine experiment at pH 7. The best results were obtained here with a 6.7% lower value of 0.350 mol/L. This indicates that the capacity of the resin may be slightly pH-dependent, which is very common for weak ion-exchange resins, but somewhat unexpected for this resin. Further research is required to verify the pH-dependence of the capacity.

Selectivities. The slopes of the breakthrough curves of the experiments in which chloride was involved indicate that the value of S_{Cl^-,OH^-} must be smaller than the value obtained from batch equilibrium experiments. The latter value was de-

Table 4. Model Parameters Used in the Simulation of the Block-Pulse Experiments

No. of spatial discretization steps	N	100
Resin capacity	Q	0.375* mol/L
Bed void fraction	ϵ	0.569
Selectivities		
Acetate/OH^-	S_{Ac^-,OH^-}	0.0253
N-Acetylmethionine anion/OH^-	S_{AcM^-,OH^-}	0.030
N-Acetylmethionine cation/H^+	S_{AcM^+,H^+}	0.565
Sodium/H^+	S_{Na^+,H^+}	1
Chloride/H^+	S_{Cl^-,OH^-}	0.075
Distribution of coefficients		
Acetic acid	K_{HAc}	1.079
N-acetylmethionine	K_{AcM}	1.423

*A value of 0.350 mol/L was used for the displacement experiment of acetate and *N*-acetylmethionine at pH 7.

termined from experiments where the pH was in general very high. Since the capacity of the resin seems to be pH-dependent to some extent, it is likely that the capacity at these very high pH values may not be compared with those under moderate pH values used in this study. This may have affected the calculation of value of the selectivity. Very good simulation results were obtained with the value given in Table 4.

The value of S_{Na^+,H^+} could not be determined accurately from batch equilibrium experiments. The height of the acetic acid plateau between the acetic acid wave and the exchange wave of acetate/*N*-acetylmethionine or acetate/chloride in the experiments at pH 5 indicated that $S_{Na^+,H^+} \approx 1$, but the parameter sensitivity was insufficient to allow a more accurate estimate from the present experiments.

On the basis of simulations of preliminary experiments (not shown) the value of S_{AcM^-,OH^-} was adjusted with 10% to give a value of the selectivity of *N*-acetylmethionine over acetate, S_{AcM^-,Ac^-}, equal to 1.2. With this value the experiments could be described very well.

pH Profiles. In general the model could describe the concentration profiles well, but apparently large deviations between model simulations and measurements were found for the pH profiles. This is illustrated by Figure 5. In this figure the rise of the pH after the introduction of *N*-acetylmethionine on the column appeared to be somewhat slower than predicted by the model, which corresponds with the simulated increase of the acetic acid, which also increased more slowly. In the simulations the pH returns to the influent value after the wave of exchange of acetate against *N*-acetylmethionine, whereas in practice the pH remains high until the end of the block pulse. This phenomenon might be due to mass-transfer limitations, and it was investigated further by changing the relative block-pulse width (see Figures 6a and 6b).

In Figure 5 the dimensionless block-pulse width was approximately 10. In the experiments to test the influence of the block-pulse width, the pulse widths of 15, 25, and 35 min correspond to dimensionless widths of approximately 7.5, 12.5, and 17.5. The concentration profiles in Figure 6a, given as the extinction at 254 nm, are as expected. They are very similar and only differ in the width of the response curve. The experimental pH profiles in Figure 6b exhibit a sudden transition. With the smallest block pulse the pH remained high until it suddenly dropped due to the shift from *N*-acetylmethionine back to acetic acid. In the case of the second block pulse the pH dropped before the end of the pulse, but it had not entirely reached the feed value when the eluent was switched back to acetic acid. Only with the widest block pulse the pH had returned to its initial value before the end of the block pulse. Apparently a dimensionless pulse width of approximately 12.5 is required to reach the steady state. This is much more than can be expected on the basis of the hydraulic residence time, which means that difference between simulated and experimental pH profiles is associated with mass-transfer limitations. Most likely the delay in the pH response is a consequence of the slow uptake or release of undissociated components. After the introduction of *N*-acetylmethionine, its anions start to displace acetate anions. Simultaneously undissociated *N*-acetylmethionine, although present only as a small fraction, is taken up by the resin. The absorption of undissociated *N*-acetylmethionine, however,

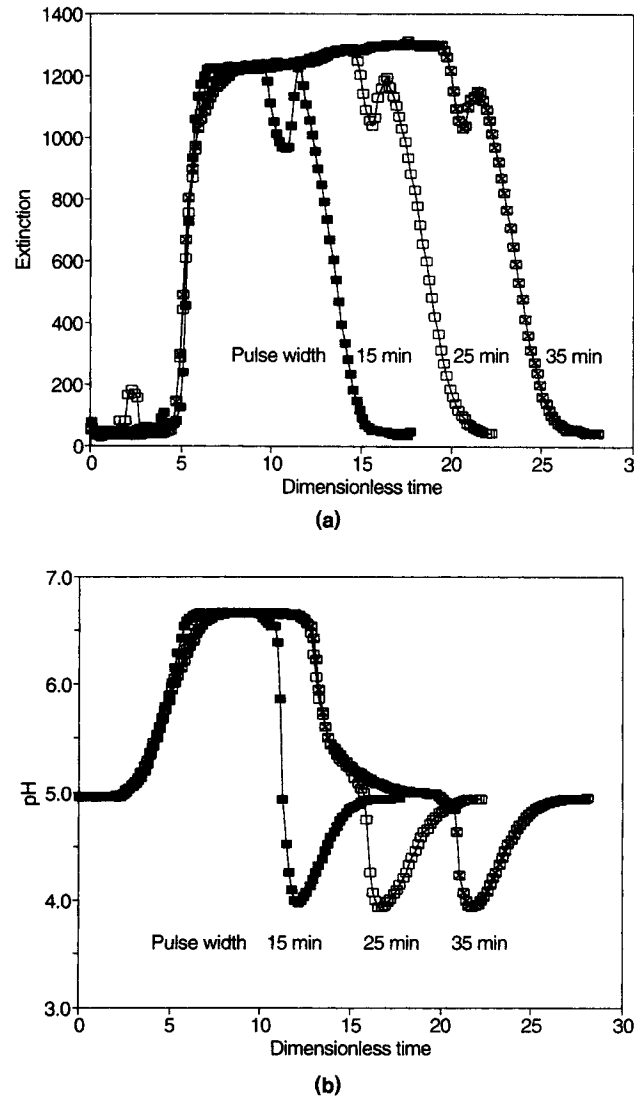

Figure 6. Experimental concentration profiles (a) and pH profiles (b) in displacement experiments of acetate and *N*-acetylmethionine at pH 5 with variable *N*-acetylmethionine block-pulse width.

disturbs the dissociation equilibrium, which is restored by the association of *N*-acetylmethionine anions with H^+. As a consequence the proton concentration decreases and the pH increases. Because the concentration of neutral *N*-acetylmethionine is low, the driving force for mass transfer is small and the absorption proceeds slowly. So the pH remains high longer than expected, and only when the entire column is in equilibrium with the feed, does the pH return to the expected value.

Although the magnitude of the pH deviation seems to be large, it is very small in terms of concentration differences. The deviation between pH 5 and the measured value of 6.5 corresponds to a difference in proton concentrations of the order of magnitude of 10^{-5} mol/L. This is 0.01% of the electrolyte concentration of 0.1 mol/L, whereas the order of magnitude of the analytical errors is 1%. Since in the simula-

tion model the proton concentration is computed by an iterative procedure from the electroneutrality equation, a relative deviation between actual and calculated ion concentrations of 0.01% could result in errors in the pH of the same order of magnitude as found in this work. All this is less relevant for buffered systems, where the pH tends to be self-correcting, but for unbuffered solutions containing, for example, only strong electrolyte ions, this is much more important. In the present study the deviations manifested themselves therefore primarily with solutions of chloride or with *N*-acetylmethionine at pH 5–6 and above.

It is not expected that the simulated concentration profiles can be improved significantly by a fixed-bed model in which mass-transfer effects and diffusion are incorporated explicitly, instead of implicitly in the apparent dispersion coefficient, because the concentration profiles are described quite well already. On the other hand, the pH profiles might be predicted better if these mass-transfer effects, which are held responsible for the deviations between experiments and simulations, are taken into account. The benefit is difficult to predict since the mass-transfer effects are apparently very small. This remains to be further examined, but it was beyond the scope of this work.

Conclusions

Secondary equilibrium, in particular dissociation equilibria, were demonstrated to be of paramount importance to ion-exchange processes in which weak electrolytes are involved. These dissociation equilibria influence the ion-exchange process in two ways. First, the actual exchange of ions is affected by the transition of a component into the neutral form, which reduces the ionic fraction and hence the competitiveness of the component compared to the other ions present. Second, the apparent affinity of a component for the resin phase is increased if in addition to the ionically bound ions the neutral species is also absorbed by the resin.

The uptake or release of neutral species leads to concentration fluctuations that are superimposed on the normal ion-exchange profiles. The concentration fluctuations are induced by the unequal concentration levels of associated ions due to variations in the extent of dissociation of different weak electrolytes. Furthermore, pH fluctuations that are inherent to the exchange of ions with different selectivities influence the extent of dissociation of the components. Consequently, the pH fluctuations affect the ionic fractions in the exchange zone, and hence indirectly act upon the concentration profiles in the effluent.

The net effect of the occurrence of neutral species is strongly dependent on the type of resin and on the experimental conditions, especially the pH, concentrations, and dissociation behavior of the weak electrolytes. The importance of the uptake of neutral species increases as the capacity of the resin is lower, as the total concentration of a component is higher and, obviously, as the fraction of the neutral species is higher. With the resin, electrolytes, and other experimental conditions applied in this work, the reduction of the anionic fraction appeared to be the dominant factor. This means that for the design of an ion-exchange chromatography process aimed at the separation of a mixture of acetic acid and *N*-acetylmethionine, the pH is the major control variable with which the fraction of acetate anions can be reduced, favoring its separation from *N*-acetylmethionine (Jansen et al., in preparation).

The simulations with the dynamic fixed-bed model, based on the DIX equilibrium model, in general fitted the experimental concentration profiles very well. Also besides taking the exchange of ions and the uptake of neutral species into account, all concentration fluctuations that were associated with the displacement of one electrolyte by another and with the (de)sorption of uncharged species could be described. The prediction of pH profiles was less satisfactory due to some apparently slow mass-transfer phenomena resulting in—in the absolute sense—small deviations of ionic concentrations, but large deviations from the experimental results in terms of H^+ and OH^- concentrations. This applies in particular to moderately buffered or unbuffered solutions, where the pH-stabilizing effect of the dissociation equilibria is absent. Nevertheless, the model is very promising for the simulation of multicomponent separations and for ion-exchange chromatography integrated with chemical reactions in which weak electrolytes are involved (Jansen et al., 1996).

Acknowledgment

Analyses were done by J. Knoll, J. B. A. van Tol, and C. Ras. Their contribution is gratefully acknowledged. The authors also wish to thank D. M. F. T. dos Prazeres and G. W. Hofland for their preliminary investigations in this field.

Notation

Superscripts and subscripts

Ac = acetate
AcM = *N*-acetylmethionine
Cl^- = chloride
H^+ = protons
HAc = acetic acid
Na^+ = sodium
OH^- = hydroxide

Literature Cited

Carta, G., M. S. Saunders, J. P. DeCarli II, and J. B. Vierow, "Dynamics of Fixed-Bed Separations of Amino Acids by Ion-Exchange," *AIChE Symp. Ser.*, **84**(264), 54 (1988).

Chibata, I., and T. Tosa, "Industrial Applications of Immobilized Enzymes and Immobilized Microbial Cells," *Applied Biochemistry and Bioengineering*, Vol. 1, *Immobilized Enzyme Principles*, L. B. Wingard, E. Katchalski-Katzir, and L. Goldstein, eds., Academic Press, New York, p. 329 (1976).

DeCarli, J. P. II, G. Carta, and C. H. Byers, "Displacement Separations by Continuous Annular Chromatography," *AIChE J.*, **36**(8), 1220 (1990).

Ermakov, S. V., M. Y. Zhukov, L. Capelli, and P. G. Righetti, "Experimental and Theoretical Study of Artifactual Peak Splitting in Capillary Electrophoresis," *Anal. Chem.*, **66**, 4034 (1994).

Fóti, G., P. Hajós, and E. sz. Kováts, "Retention in Analytical Ion Exchange Chromatography—I. Strong Electrolytes on Strong Ion Exchangers," *Talanta*, **41**, 1073 (1994).

Golshan-Shirazi, S., and G. Guiochon, "The Equilibrium-Dispersive Model of Chromatography," *Theoretical Advancement in Chromatography and Related Separation Techniques, NATO ASI Ser. C*, Vol. 383, F. Dondi and G. Guiochon, eds., Kluwer, Dordrecht, The Netherlands, p. 35 (1992).

Guiochon, G., S. Golshan-Shirazi, and A. M. Katti, *Fundamentals of Preparative and Nonlinear Chromatography*, Chaps. II, VI, X, XI, Academic Press, Boston (1994).

Helfferich, F. G., *Ion Exchange*, McGraw-Hill, New York, p. 95 (1962).
Helfferich, F. G., "Ion-Exchange Equilibria of Amino Acids on Strong-Acid Resins: Theory," *React. Poly.*, **12**, 95 (1990).
Helfferich, F. G., and B. J. Bennett, "Weak Electrolytes, Polybasic Acids, and Buffers in Anion Exchange Columns I. Sodium Acetate and Sodium Carbonate Systems," *React. Poly.*, **3**, 51 (1984a).
Helfferich, F. G., and B. J. Bennett, "Weak Electrolytes, Polybasic Acids, and Buffers in Anion Exchange Columns II. Sodium Acetate Chloride Systems," *Solvent Extr. Ion Exch.*, **2**(7,8), 1151 (1984b).
Jansen, M. L., A. J. J. Straathof, L. A. M. van der Wielen, K. Ch. A. M. Luyben, and W. J. J. van den Tweel, "A Rigorous Model for Ion Exchange Equilibria of Strong and Weak Electrolytes," *AIChE J.*, **42**, 1911 (1996a).
Jansen, M. L., G. W. Hofland, J. Houwers, A. J. J. Straathof, L. A. M. van der Wielen, K. Ch. A. M. Luyben, and W. J. J. van den Tweel, "Effect of pH and Concentration on Column Dynamics of Weak Electrolyte Ion Exchange Processes," *AIChE J.*, **42**, 1925 (1996b).
Jansen, M. L., E. van Zessen, A. J. J. Straathof, L. A. M. van der Wielen, K. Ch. A. M. Luyben, and W. J. J. van den Tweel, "Immobilisation of Aminoacylase on an Anion Exchange Column to be Used as a Chromatographic Reactor," *Ann. N.Y. Acad. Sci.*, in press (1996c).
Jones, I. L., and G. Carta, "Ion Exchange of Amino Acids and Dipeptides on Cation Resins with Varying Degree of Cross-Linking. 1. Equilibrium," *Ind. Eng. Chem. Res.*, **32**, 107 (1993).
Kawakita, T., and T. Matsuishi, "Elution Kinetics of Lysine from a Strong Cation-Exchange Resin with Ammonia Water," *Sep. Sci. Technol.*, **26**(7), 991 (1991).
Karger, B. L., J. N. LePage, and N. Tanaka, "Secondary Chemical Equilibria in High-Performance Liquid Chromatography," *High-Performance Liquid Chromatography. Advances and Perspectives*, C. Horváth, ed., Vol. 1, Academic Press, New York, p. 113 (1980).
Keller, R. A., and J. C. Giddings, "Multiple Zones and Spots in Chromatography," *J. Chromag.*, **3**, 205 (1960).
Kitakawa, A., T. Yonemoto, and T. Tadaka, "A Mathematical Model for the Separation of Amino Acids Using Ion Exchange Chromatography," *Trans. Ind. Chem. Eng.*, **72**(C), 201 (1994).
Klein, G., "Ion-Exchange and Chemical Reaction in Fixed Beds," *Percolation Processes: Theory and Applications*, A. E. Rodrigues and D. Tondeur, eds., Sijthoff & Noordhoff, Alphen aan den Rijn, The Netherlands, p. 363 (1981).
Mehablia, M. A., D. C. Shallcross, and G. W. Stevens, "Prediction of Multicomponent Ion Exchange Equilibria," *Chem. Eng. Sci.*, **49**, 2277 (1994).
Myers, A. L., and S. Byington, "Thermodynamics of Ion Exchange: Prediction of Multicomponent Equilibria from Binary Data," *Ion Exchange Technology*, A. E. Rodrigues, ed., Nijhoff, Dordrecht, The Netherlands, p. 119 (1986).
Saunders, M. S., J. B. Vierow, and G. Carta, "Uptake of Phenyalanine and Tyrosine by a Strong-Acid Cation Exchanger," *AIChE J.*, **35**(1), 53 (1989).
Tao, Z., "Ion-Exchange Equilibria of Amino Acids," *Ion Exch. Solvent Extr.*, **12**, 353 (1995).
Wandrey, C., and E. Flaschel, "Process Development and Economic Aspects in Enzyme Engineering. Acylase L-Methionine System," *Adv. Biochem. Eng.*, **12**, 147 (1979).

Appendix: Relation Between Resin-Phase Dissociation Constant and Overall Distribution Coefficient

Taking acetic acid as an example, the overall distribution coefficient of the neutral species is defined according to Eq. 5 as follows:

$$K_{\mathrm{HAc}} = \frac{c^R_{\mathrm{HAc}}}{c^L_{\mathrm{HAc}}}. \tag{A1}$$

The dissociation constant is defined as follows:

$$K_a = \frac{c_{\mathrm{H}^+} c_{\mathrm{Ac}^-}}{c_{\mathrm{HAc}}}. \tag{A2}$$

This equation applies to both liquid and resin phases. Now the overall distribution coefficient can be expressed in terms of ionic concentrations and dissociation constants:

$$K_{\mathrm{HAc}} = \frac{K^L_a}{K^R_a} \cdot \frac{c^R_{\mathrm{H}^+} c^R_{\mathrm{Ac}^-}}{c^L_{\mathrm{H}^+} c^L_{\mathrm{Ac}^-}}. \tag{A3}$$

The ratios of resin- and liquid-phase concentrations of H^+ and Ac^- can be substituted by the expressions from the DIX model. After some minor rearrangements this results in the following expression for the overall distribution coefficient:

$$K_{\mathrm{HAc}} = \frac{K^L_a}{K^R_a} \cdot S_{\mathrm{Ac}^-,\mathrm{OH}^-}. \tag{A4}$$

As expected, the resin capacity does not affect the uptake of neutral species. A high value of K_a in the liquid phase (high degree of dissociation) and a low value in the resin phase (low degree of dissociation) favor the presence of neutral acetic acid in the resin phase. A high value for the anion selectivity also favors the uptake of neutral species indirectly: it enhances the uptake of anions, and to maintain the dissociation equilibrium, neutral species must then be absorbed as well.

Manuscript received Apr. 17, 1996, and revision received June 21, 1996.